# $CTDI_{vol}$ : a suitable normalization for CT dose conversion coefficients at different tube voltages?

Helmut Schlattl, Maria Zankl and Christoph Hoeschen

Helmholtz Zentrum München – German Research Center for Environmental Health, Research Unit Medical Radiation Physics and Diagnostics, Ingolstädter Landstr. 1, 85764 Neuherberg

#### **ABSTRACT**

Reliable estimates of patient doses for CT examinations are desirable for the patients themselves as well as for new epidemiological studies. It has been shown that dose conversion coefficients normalized to  $\mathrm{CTDI_{vol}}$  provide rather scanner independent quantities. In this work, it is demonstrated that this normalization provides also tube voltage independent values by simulating axial CT scans of a seven-year old infant and an adult. The differences in the effective dose conversion coefficients per  $\mathrm{CTDI_{vol}}$  between 80 and 120 kV is for most body regions below 5%. Only at the height of the testes and the thyroid the difference can be as large as 15%. This results in differences of the effective dose conversion coefficient per  $\mathrm{CTDI_{vol}}$  between 80 and 120 kV of less than 6-7% for typical CT examinations.

#### 1. INTRODUCTION

The increasing usage of computed tomography and the relatively large doses connected with this imaging modality compared to other techniques led to an increasing concern about late-time detrimental effects. In this context, it is of particular interest for the patients to get informed about their actual organ and/or effective doses received during such a procedure. Moreover, to improve the cancer-risks estimations at low levels of radiation, new cohorts for a long-term follow-up of patients after CT exams are desirable. In such studies reliable estimates of the patient organ and effective doses are required.

Patient organ doses can only be obtained numerically by simulating the imaging process, usually employing Monte Carlo methods. The result of such simulations are organ doses related to an externally measurable quantity like air kerma. For CT, an appropriate reference quantity is the weighted  ${\rm CTDI_w}$ , or for spiral scans  ${\rm CTDI_{vol}}$  which accounts for different pitch settings. This quantity is known to have limitations, in particular, with larger number of detector rows to estimate the patient doses directly, but is nonetheless a suitable normalization quantity for numerical dose conversion coefficients in CT. It has been shown that organ dose conversion coefficients normalized to  ${\rm CTDI_{vol}}$  are relatively insensitive to the scanner type. In this work, we are addressing how strong organ dose conversion coefficients per  ${\rm CTDI_{vol}}$  depend on the tube voltage settings for one particular CT device using voxel models of an infant and an adult. With all CT devices providing this quantity for each CT exam,  ${\rm CTDI_{vol}}$  could be a very suitable normalization quantity for CT dose conversion coefficients.

#### 2. MATERIALS AND METHODS

## 2.1 Voxel models and Monte Carlo simulations

The voxel models employed are "Child"<sup>5</sup> and the male adult ICRP/ICRU reference computational model,<sup>6</sup> denoted as "RCP-AM" (see Fig. 1). The main properties of both models are summarized in Table 1. Child is based on CT images of a seven-year old infant, and compared to its original version<sup>5</sup> has been meanwhile revised and has now 125 explicitly segmented organs. To compute the effective dose as defined in ICRP Publication 103<sup>7</sup> almost all organs are present in Child. Exceptions are the endosteum and the lymphatic nodes, the doses of which are estimated by the surrogate organs spongiosa and residual tissue, respectively.

The simulations have been performed using EGSnrc in version V4-2-3-0.8 The paths of photons and (secondary) electrons were followed until their energies falls below 2 and 20 keV, respectively. Rayleigh scattering, Photo effect and

Correspondence to H.S. (helmut.schlattl@helmholtz-muenchen.de)



Figure 1. Images of the models used where breast, bones, colon, eyes, lungs, liver, pancreas, small intestine, stomach, teeth, thyroid and urinary bladder can be identified by different surface colors. Muscle and adipose tissue are made transparent. For illustration purposes the voxelized surfaces have been smoothed.

bound Compton scattering were considered. Details of the physics and particle transport scheme conform with those described in an earlier publication.<sup>9</sup>

The shape and thickness of the x-ray filtration used in the simulations corresponds to a Siemens Sensation Cardiac 16 (Siemens Medical Solutions, Forchheim, Germany) with focus to isocenter distance of 57 and a field of view of 50 cm at the isocenter distance.\* Simulations with tube voltages of 80 and 120 kV have been performed. The x-ray tube spectra have been determined using the program SpekCalc.<sup>10</sup>

Table 1. Selected properties of employed voxel models.

Model	Age	Height	Weight	Voxel dimensions
		(cm)	(kg)	$(\text{mm}^3)$
RCP-AM	_	176	73	$2.137 \times 2.137 \times 8$
Child	7 yr	115	21.7	$1.54\times1.54\times8$

## 2.2 CTDI-to-air-kerma ratios

In numerical dosimetry the organ doses are normalized usually to air kerma at certain locations. In this work, air kerma at the rotation axis ( $K_a$ ) is used. To relate  $K_a$  to a CT dose index, axial scans of a CTDI body phantom with diameter of 32 cm were simulated. The virtual CTDI body phantom has a height of 15 cm and consists of PMMA with a density of 1.10 g/cm<sup>3</sup> with one hole at the center and 4 holes near the edge with a diameter of 1 cm each. The centers of the 4 peripheral holes are located 1 cm from the edge of the phantom. Each hole has a height of 10 cm, is filled with air, and is covered with

<sup>\*</sup>Details of filter material and shape are the proprietary of the manufacturer and cannot be disclosed.

2.5 cm of perspex. Four axial scans with collimations of 2, 5, 10, and 16 cm have been performed to quantify the influence of the collimation on the ratios of different CTDI-values to air kerma at the rotation axis. By integrating the doses in the central and peripheral holes over 10 cm and and dividing them by the scan length,  $\text{CTDI}_{100}^{\text{c}}/K_{\text{a}}$  and  $\text{CTDI}_{100}^{\text{p}}/K_{\text{a}}$  are determined. The weighted CTDI values are then given by the well known formula

$$CTDI_{w} = \frac{1}{3}CTDI_{100}^{c} + \frac{2}{3}CTDI_{100}^{p}.$$

In these simulations, the history of  $2 \times 10^9$  photons has been followed, which resulted in a relative statistical uncertainty of at most about 4 and 2% for  $\mathrm{CTDI}_{100}^{\mathrm{c}}/K_{\mathrm{a}}$  and  $\mathrm{CTDI}_{100}^{\mathrm{p}}/K_{\mathrm{a}}$ , respectively.

## 2.3 Dose conversion coefficients

Simulating each CT examination with specific collimations, pitch settings, scan regions, etc. is very CPU time consuming. Therefore, it is common practice not to simulate the each CT examination in detail, but instead simulate sets of axial slices. By combining the resulting dose conversion coefficients of those axial slices which are within the scan region, the actual conversion coefficients for each CT examination can be deduced. It has been shown that the difference between using this method and simulating the helical trajectory in detail are small. For sets of axial scans with collimation  $h_{\rm col}$  centered at  $z_j^a$  with  $z_j^a - z_{j-1}^a = h_{\rm col}$ , the dose conversion coefficients for a scan between  $z_l$  and  $z_u$  ( $z_l < z_u$ ) are then given by

$$DCC_{ax}^{K}(z_{l}, z_{u}) = \frac{\sum_{j=jl}^{ju} w_{j} DCC_{ax,j}^{K} K_{a,j}}{\sum_{j=jl}^{ju} w_{j} K_{a,j}},$$
(1)

where  $DCC_{ax,j}^K$  is the dose conversion coefficient normalized to air kerma at the rotation axis  $(K_a)$  of axial (ax) slice j. The summation is performed over all j that fulfill

$$z_j^a + h_{\rm col}/2 \ge z_l$$
 and  $z_j^a - h_{\rm col}/2 \le z_u$ . (2)

To account for incomplete coverage of slices at the edge of the scan region, weights  $w_i$  are defined as

$$w_j = \frac{1}{2} + \begin{cases} (z_j^a - z_l)/h_{\text{col}} & \text{for } j = jl\\ (z_u - z_j^a)/h_{\text{col}} & \text{for } j = ju\\ 1/2 & \text{otherwise.} \end{cases}$$
 (3)

Using the relation  $N_{\rm R} \Psi h_{\rm col} = z_u - z_l$  ( $\Psi$ : pitch,  $N_{\rm R}$ : number of rotations), organ dose conversion coefficients normalized to  ${\rm CTDI_{vol}}$  ( $DCC^{\rm CT}$ ) are then given by

$$DCC^{\text{CT}} = DCC_{\text{ax}}^K \left(\frac{\text{CTDI}_{\text{w}}}{K}\right)^{-1} \frac{z_u - z_l}{h_{\text{col}}}$$
(4)

where  $\mathrm{CTDI_w}/K_a$  is determined numerically (see Sect. 2.2). It should be noted that in Eq. (4) only  $\mathrm{CTDI_w}/K_a$  is depending on the actual collimation used in a specific scan.

In this formalism, overscanning (or overranging) in spiral mode is incorporated by adjusting  $z_l$  and  $z_u$  accordingly. Effective dose conversion coefficients are computed by weighting the individual organ dose conversion coefficients following the definition of ICRP Publication 103.<sup>7</sup> It should be noted that these dose conversion coefficients are not to be used for risk estimations but are intended to demonstrate the impact of the tube voltage on a "mean" dose quantity.

In all simulations, axial slices with  $h_{\rm col}=5\,\mathrm{mm}$  and tube voltages of 80 and 120 kV have been simulated covering the whole body. The number of photon histories was 40 million per slice yielding statistical uncertainties of less than 0.1% for  $DCC_8^{\rm CT}$  of organs within the primary field.

The set of  $DCC_{\mathrm{ax},j}^K$  has been used to compute effective  $DCC_8^{\mathrm{CT}}$  for axial slice with collimation of 5 mm ( $h_{\mathrm{col}}=z_u-z_l$ ), and for exemplary CT examinations using Eq. (4). The scan ranges of these CT examinations are summarized in Table 2.

Table 2. Start position  $(z_u)$  and scan range  $(\Delta z = z_u - z_l)$  for a selection of CT examinations of Child and RCP-AM in cm. The start position is measured relative to the bottom of the phantom. The parameters are determined using the landmarks specified in a German CT survey.<sup>11</sup>

	Cl	hild	RCP-AM		
	$z_u$	$\Delta z$	$z_u$	$\Delta z$	
Face/neck	103.2	10.4	164.8	17.6	
Chest	95.2	14.4	150.4	24.8	
Abdomen/pelvis	84.8	31.2	131.2	45.6	
Lumbar spine	76.8	13.6	120.0	16.8	
While trunk	96.0	44.0	150.4	64.8	

## 3. RESULTS AND DISCUSSION

## 3.1 CTDI-to-air-kerma ratios

The influence of the collimation on  $\mathrm{CTDI}_{100}^{\mathrm{c}}/K_{\mathrm{a}}$ ,  $\mathrm{CTDI}_{100}^{\mathrm{p}}/K_{\mathrm{a}}$  and thus  $\mathrm{CTDI}_{\mathrm{w}}/K_{\mathrm{a}}$  is illustrated in Table 3. For  $h_{\mathrm{col}}$  less than 10 cm the differences in  $\mathrm{CTDI}_{100}^{\mathrm{p}}/K_{\mathrm{a}}$  and  $\mathrm{CTDI}_{100}^{\mathrm{c}}/K_{\mathrm{a}}$  are close or below the  $1\,\sigma$  statistical uncertainty of at most 2 and 4%, respectively, although a tendency for a small decrease with increasing collimation can be observed. At  $h_{\mathrm{col}}=16\,\mathrm{cm}$  not all primary radiation can be recorded by the 10 cm long dosimeters, particularly by the central dosimeters. In the peripheral position the largest contribution of the dose recordings are from positions, when the holes are closest to the source, i.e., where the effective collimation can be up to  $57/(57-15)\approx 1.36\,\mathrm{times}$  smaller than  $h_{\mathrm{col}}$ . It could therefore be expected that the difference in  $\mathrm{CTDI}_{100}^{\mathrm{p}}/K_{\mathrm{a}}$  between  $h_{\mathrm{col}}=2\,\mathrm{cm}$  and  $16\,\mathrm{cm}$  are smaller than in  $\mathrm{CTDI}_{100}^{\mathrm{c}}/K_{\mathrm{a}}$ , which can, however, not be confirmed. The reason is that the contribution of scatter radiation is higher for the central than for the peripheral dosimeters. Since scatter radiation originates from regions with smaller effective collimation, i.e., closer to the source than the center, less scattered than primary photons are missed by the 10 cm long central dosimeters for  $h_{\mathrm{col}}=16\,\mathrm{cm}$ . It is worth noticing that the contribution of scatter radiation to  $\mathrm{CTDI}_{100}^{\mathrm{p}}/K_{\mathrm{a}}$  and  $\mathrm{CTDI}_{100}^{\mathrm{c}}/K_{\mathrm{a}}$  is about 50 and 85%, respectively, for  $h_{\mathrm{col}}=2\,\mathrm{cm}$ .

In summary, since  $\mathrm{CTDI}_{100}^{\mathrm{c}}/K_{\mathrm{a}}$  and  $\mathrm{CTDI}_{100}^{\mathrm{p}}/K_{\mathrm{a}}$  remains rather constant for  $h_{\mathrm{col}} \leq 10\,\mathrm{cm}$ , it is justified to use for these collimations only one value for  $\mathrm{CTDI_{w}}/K_{\mathrm{a}}$  in Eq. (4). In these cases  $DCC^{\mathrm{CT}}$  becomes independent of the collimation. For larger collimations, using the same value for  $\mathrm{CTDI_{w}}/K_{\mathrm{a}}$  would underestimate the dose by at most about 20% (for  $h_{\mathrm{col}} = 16\,\mathrm{cm}$ ).

## 3.2 Dose conversion coefficients

For each slice covering the voxel models Child and RCP-AM respectively, the effective  $DCC^{CT}$  has been computed using Eq. (4) with  $h_{col} = z_u - z_l$ , i.e, for an axial slice with collimation of 5 mm. The relative difference of the effective  $DCC_s^{CT}$  at 80 kV compared to those at 120 kV are shown in Fig. 2 for Child and RCP-AM. Apart from a few positions, the relative differences are below a few percent and smaller for Child than for RCP-AM. Thus, the weighting of central to peripheral dose of 1/2 in the definition of  $CTDI_w$  reproduces rather well the dependence of the effective dose on the tube potential.

Table 3. Ratios of CTDI to air kerma on rotation axis (in mGy/mGy) for different collimations  $h_{col}$  (in cm) and tube voltages using the CTDI body phantom. The %-columns contain the relative deviations (in %) from the analogue values at  $h_{col} = 2 \text{ cm}$ .

80 kV					120 kV								
$h_{\rm col}$	$\frac{\text{CTDI}_{100}^{\text{c}}}{K_{\text{a}}}$	(%)	$\frac{\text{CTDI}_{100}^{\text{p}}}{K_{\text{a}}}$	(%)	$\frac{\text{CTDI}_{\text{w}}}{K_{\text{a}}}$	(%)		$\frac{\text{CTDI}_{100}^{\text{c}}}{K_{\text{a}}}$	(%)	$\frac{\text{CTDI}_{100}^{\text{p}}}{K_{\text{a}}}$	(%)	$\frac{\text{CTDI}_{\text{w}}}{K_{\text{a}}}$	(%)
2.0	0.113		0.257		0.209			0.163		0.309		0.261	
5.0	0.105	-7	0.259	1	0.208	-1		0.158	-3	0.303	-2	0.255	-2
10.0	0.108	-4	0.249	-3	0.202	-3		0.155	-5	0.294	-5	0.248	-5
16.0	0.089	-21	0.203	-21	0.165	-21		0.118	-28	0.243	-21	0.201	-23

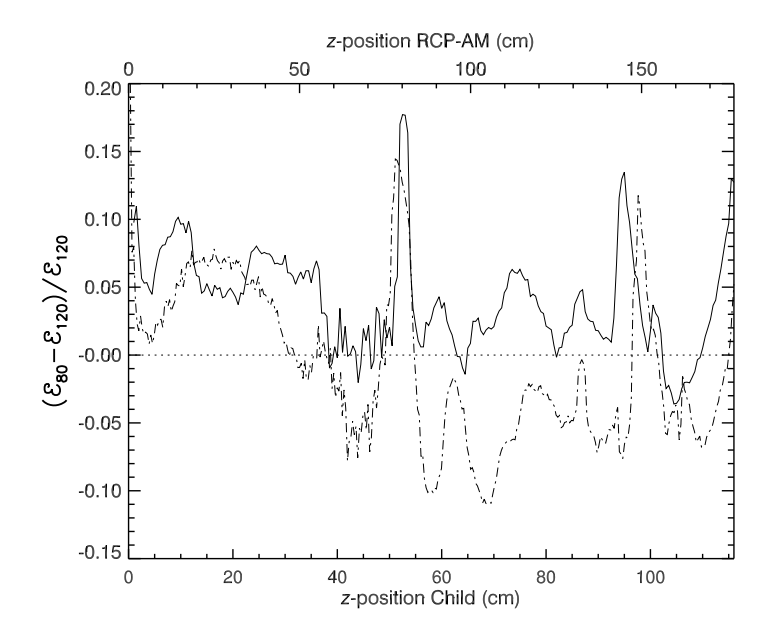


Figure 2. Relative difference of the effective  $DCC^{CT}$  ( $\mathcal{E}$ ) at 80 kV to the effective  $DCC^{CT}$  at 120 kV for different slice positions in Child (solid line) and RCP-AM (dashed line).

The largest difference are observed for both phantoms at the height of the testes (Child:  $z\approx 50\,\mathrm{cm}$ , RCP-AM:  $z\approx 80\,\mathrm{cm}$ ) and the thyroid (Child:  $z\approx 95\,\mathrm{cm}$ , RCP-AM:  $z\approx 145\,\mathrm{cm}$ ). Both organs are located rather off-center, and thus the central-to-peripheral weighting in  $\mathrm{CTDI_w}$  can only poorly describe the dependence of these organ doses with the tube voltage.

To quantify, how these difference translate into  $DCC_s^{\rm CT}$  of actual CT examinations, effective  $DCC_s^{\rm CT}$  for a selection of typical CT scans are summarized in Table 4. As expected, the difference are even smaller than those for individual slice, thus confirming that the dependence of the effective  $DCC_s^{\rm CT}$  on the tube voltage can be neglected.

## 4. CONCLUSIONS

The dependence of patient effective dose conversion coefficients for CT scans normalized to  $\mathrm{CTDI_{vol}}$  on the applied tube voltages is shown using pediatric and adult human models. Effective dose conversion coefficients normalized to  $\mathrm{CTDI_{vol}}$  show only a weak dependence on the tube voltages for both pediatric as well as adult patients. For single axial slices the effective  $DCC_s^{\mathrm{CT}}$  at 80 and 120 kV differ at most about 15% for both phantoms. For typical CT examinations the relative difference is less than 7%. Considering in addition the weak dependence of  $DCC^{\mathrm{CT}}$  on the specific scanner,<sup>4</sup> normalizing dose conversion coefficient to  $\mathrm{CTDI_{vol}}$  offers the possibility to deduce reliable patient doses from a limited set of conversion coefficients. For collimations larger than 10 cm the effective doses can be underestimated by at most

Table 4. List of effective  $DCC_8^{\rm CT}$  in mSv/mGy for different CT examinations at 80 and 120 kV. For each phantom, the deviation of the effective  $DCC^{\rm CT}$  at 120 kV from that at 80 kV is provided in the respective  $3^{\rm rd}$  column.

		Child		RCP-AM			
Examination	$80\mathrm{kV}$	$120\mathrm{kV}$	(%)	$80\mathrm{kV}$	$120\mathrm{kV}$	(%)	
Face/neck	0.36	0.33	-7.	0.26	0.25	-3.	
Chest	0.99	0.95	-4.	0.76	0.78	3.	
Abdomen/pelvis	1.60	1.55	-3.	0.85	0.90	5.	
Lumbar spine	0.76	0.74	-4.	0.27	0.28	5.	
Whole trunk	2.52	2.41	-4.	1.43	1.48	4.	

about 20% for the currently used largest collimation of 16 cm. It remains to be investigated how strong this value depends on the scanner type used, i.e., on the different bowtie filters employed. But it is expected that the dependence is rather weak, such that only one set of collimation-dependent correction factors will be necessary for  $h_{\rm col} > 10$  cm.

It is worth noticing that the difference in organ  $DCC_8^{\rm CT}$  between 80 and 120 kV is larger than for the effective  $DCC_8^{\rm CT}$ . Thus, for a more detailed investigation of organ doses, it will not suffice to use a single set of organ  $DCC_8^{\rm CT}$ . But, there are other factors influencing the individual patient organ doses like patient stature, organ location and/or tube current modulation, which then have to be considered too.<sup>9</sup>

#### REFERENCES

- [1] Brenner, D. J., Elliston, C. D., Hall, E. J. and Berdon, W. E., "Estimated risks of radiation-induced fatal cancer from pediatric CT," Am. J. Roentgenol.176(2), 289–296 (2001).
- [2] Committee to Assess Health Risks from Exposure to Low Levels of Ionizing Radiation, [Health Risks from Exposure to Low Levels of Ionizing Radiation: BEIR VII Phase 2], The National Academic Press, Washington, USA (2006).
- [3] Kyriakou, Y., Deak, P., Langner, O. and Kalender, W. A., "Concepts for dose determination in flat-detector CT," Phys. Med. Biol.53(13), 3551 (2008), doi:10.1088/0031-9155/53/13/011.
- [4] Turner, A. C., Zankl, M., DeMarco, J. J., Cagnon, C. H., Zhang, D., Angel, E., Cody, D. D., Stevens, D. M., McCollough, C. H. and McNitt-Gray, M. F., "The feasibility of a scanner-independent technique to estimate organ dose from MDCT scans: Using CTDI<sub>vol</sub> to account for differences between scanners," Med. Phys.37(4), 1816–1825 (2010), doi:10.1118/1.3368596.
- [5] Zankl, M., Veit, R., Williams, G., Schneider, K., Fendel, H., Petoussi, N. and Drexler, G., "The construction of computer tomographic phantoms and their application in radiology and radiation protection," Radiat. Environ. Biophys.27(2), 153–164 (1988), doi:10.1007/BF01214605.
- [6] International Commission on Radiological Protection, [Adult reference computational phantoms], ICRP Publication 110, Elsevier, Amsterdam, The Netherlands (2009).
- [7] International Commission on Radiological Protection, [2007 Recommendations of the International Commission on Radiological Protection], ICRP Publication No 103, Elsevier, Amsterdam, The Netherlands (2007).
- [8] Kawrakow, I., Mainegra-Hing, E., Rogers, D. W. O., Tessier, F. and Walters, B. R. B., [The EGSnrc code system: Monte Carlo simulation of electron and photon transport], PIRS Report 701, 5th printing, National Research Council of Canada, Ottawa, Canada (2010), http://irs.inms.nrc.ca/software/egsnrc/documentation/pirs701.pdf.
- [9] Schlattl, H., Zankl, M. and Hoeschen, C., "Dose conversion coefficient for CT examinations of adults with automatic tube current modulation.," Phys. Med. Biol.55, 6243–6261 (2010), doi:10.1088/0031-9155/55/20/013.
- [10] Poludniowski, G., Landry, G., DeBlois, F., Evans, P. M. and Verhaegen, F., "SpekCalc: a program to calculate photon spectra from tungsten anode x-ray tubes," Phys. Med. Biol.54(19), N433–N438 (2009), doi:10.1088/0031-9155/54/19/N01.
- [11] Brix, G., Nagel, H. D., Stamm, G., Veit, R., Lechel, U., Griebel, J. and Galanski, M., "Radiation exposure in multi-slice versus single-slice spiral CT: results of a nationwide survey," Eur. Radiol.13(8), 1979–1991 (2003), doi: 10.1007/s00330-003-1883-y.